

# REMOVING RING ARTIFACTS IN CBCT IMAGES VIA GENERATIVE ADVERSARIAL NETWORK

Shuyang Zhao<sup>1</sup>    Jianwu Li<sup>\*1</sup>    Qirun Huo<sup>2</sup>

<sup>1</sup> Beijing Key Laboratory of Intelligent Information Technology, Beijing 100081, China  
School of Computer Science and Technology, Beijing Institute of Technology  
<sup>2</sup> College of Information Engineering, Capital Normal University, Beijing 100081, China

## ABSTRACT

Cone-beam computed tomography (CBCT) images often have some ring artifacts because of the inconsistent response of detector pixels. Removing ring artifacts in CBCT images without impairing the image quality is critical for the application of CBCT. In this paper, we explore this issue as an “adversarial problem” and propose a novel method to eliminate ring artifacts from CBCT images by using an image-to-image network based on Generative Adversarial Network (GAN). Through combining the generative adversarial loss and the proposed smooth loss, both of the generator and the discriminator can be trained to remove ring artifacts in CBCT images by means of image-to-image. Experimental results demonstrate that the proposed method is more effective on both simulated data and real-world CBCT images, compared with other algorithms.

**Index Terms**— CBCT images, ring artifacts, generative adversarial network (GAN), generative adversarial loss

## 1. INTRODUCTION

As a branch of important bio-imaging, Cone Beam Computed Tomography (CBCT) has many advantages such as the high utilization ratio of rays, precise imaging. And it has been widely applied to the 3D implants, clinical diagnosis, and other medical fields. However, due to the limitations of the imaging technology [1], CBCT images often have a series of concentric ring artifacts with different gray levels from the surrounding pixels. The occurrence of ring artifacts seriously affects the authenticity and quality of CBCT images, and further interferes with the clinical diagnosis and treatment.

In the past few years, the research on ring artifacts correction has achieved great progress in the field of image processing. A number of methods have been proposed to eliminate ring artifacts and they can be roughly divided into two major categories [2]: pre-processing methods based on the pro-

jection sinogram and post-processing methods based on the reconstruction image.

Pre-processing methods are performed on the projection sinogram [3], in which ring artifacts appear as parallel vertical lines. C. Raven et al. [4] used a low-pass filter to remove the artifacts by applying Fourier transform to the projection sinogram. M. Boin et al. [5] removed artifacts during the reconstruction by using an average filter. B. Munch et al. [6] combined wavelet decomposition and Fourier low-pass filter to eliminate the artifacts. However, for the pre-processing methods, it is not easy to set the related parameters and the projection sinograms program needs the large memory space. Therefore, post-processing methods based on reconstructed images have been paid more attention.

Post-processing approaches are directly applied to the reconstructed images to reduce artifacts. [7] and [8] proposed to remove ring artifacts by using the morphological operators. A ring artifact correction method for high-resolution micro CBCT was presented in [9] and [10], which is based on the mean and median filterings of the reconstructed image and worked on a transformed version of the reconstructed image in polar coordinates. Through a linear transformation, independent component analysis (ICA) [11] was used to decompose the complex image data into different independent components, and only components containing streak artifacts were selected to be filtered. [12] proposed to use wavelet transform-FFT-Gaussian filtering on the reconstructed image for ring artifact correction. Recently, in [13], a variation-based destriping model was proposed to remove artifacts, which includes an  $L_1$ -norm-based data fidelity term and an  $L_0$ -norm/ $L_1$ -norm unidirectional variation-based regularization term. The existing post-processing methods mostly remove artifacts by different filters, and the reconstructed images need to be corrected in polar coordinates. Interpolation is often used to compensate the transformed image during the coordinate transformation so that it is inevitable to result in loss of details and blurred edges in the image.

Recently, Generative Adversarial Networks (GAN) [14] demonstrated state-of-the-art performance in many vision tasks by making an adversarial process alternating between

\*Corresponding author: ljw@bit.edu.cn (Jianwu Li). This work was supported in part by the National Natural Science Foundation of China (No.61271374).

faking and identifying, and the generative adversarial loss was designed to evaluate the discrepancy between the generated distribution and the real-world distribution. In order to suppress artifacts in the output images, we proposed a joint loss strategy, which joints the target loss and the generative adversarial loss as a new loss function. In this paper, we explore this issue as an ‘‘adversarial problem’’ and propose a novel method to gradually remove ring artifacts from CBCT images by using an image-to-image network based on GAN.

**Contributions:** The contributions of this work are three-fold.

(1) Removing ring artifacts in CBCT images in the Cartesian coordinate system directly, so as to avoid the loss of image details resulting from the coordinate transformation from the Cartesian coordinate to the polar coordinate, which happened in traditional post-processing methods.

(2) Using Generative Adversarial Networks to remove ring artifacts in CBCT images.

(3) Introducing the smooth loss and further combining the smooth loss and the generative adversarial loss into GAN, (we call it Smooth GAN).

## 2. THE PROPOSED METHOD

In this section, Smooth Generative Adversarial Network (SGAN) was proposed to remove ring artifacts (Fig.1). Firstly, we explain the proposed smooth loss and the generative adversarial loss, respectively. Then we introduce the whole framework of the proposed SGAN and illustrate the details of the network architecture.

### 2.1. Smooth Loss

The CBCT image that contains artifacts can be expressed mathematically as

$$I(x, y) = S(x, y) + n(x, y), \quad (1)$$

where  $I(x, y)$  is the CBCT image in coordinates, which is the treated image containing artifacts,  $S(x, y)$  represents the ideal image without artifacts, and  $n(x, y)$  is the artifacts information in the CBCT image.

The gradient map can visually represent the smoothness of the image, as shown on the left in Fig.2 (a). The artifacts in the brain CBCT image are very unsmooth and have the concentric circles of noises. Calculating the partial derivative of Eq.(1) in  $x$  and  $y$  directions to get the gradients in the  $x$  and  $y$  directions, respectively

$$\begin{cases} \partial_x I(x, y) = \partial_x S(x, y) + \partial_x n(x, y) \\ \partial_y I(x, y) = \partial_y S(x, y) + \partial_y n(x, y) \end{cases} \quad (2)$$

In order to make sure the image is smooth enough, the objective functions can be written as

$$\min \partial_x n(x, y) = \min \left( \sum \partial_x I - \partial_x S \right)^2 \quad (3)$$

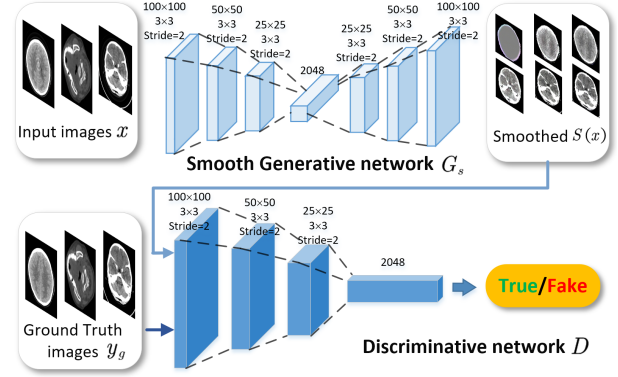


**Fig. 1.** The general framework of the proposed method.

$$\min \partial_y n(x, y) = \min \left( \sum \partial_y I - \partial_y S \right)^2 \quad (4)$$

Similarly, in order to retain the main information of the image during smoothing, it is necessary to ensure the similarity between the smoothed image and the original input image. So the loss function can be designed as

$$\min_S \left( \lambda_1 \sum_p (\partial_x S_p - \partial_x I_p)^2 + \lambda_2 \sum_p (\partial_y S_p - \partial_y I_p)^2 \right) \quad (5)$$

where  $p$  indexes 2D pixels,  $\lambda_1$  is the regularization parameter that quantifies the smoothness of  $x$  direction, and  $\lambda_2$  is the regularization parameter that quantifies the smoothness of  $y$  direction.  $\partial_x$  and  $\partial_y$  denote the  $x$  and  $y$  derivative operators, respectively. In this minimization model,  $\lambda_1 \sum_p (\partial_x S_p - \partial_x I_p)^2$  and  $\lambda_2 \sum_p (\partial_y S_p - \partial_y I_p)^2$  are two fidelity terms which ensure the smoothed image  $S$  is similar to the original image  $I$  as much as possible. And they are used to smooth the image in both the vertical and horizontal directions.

### 2.2. Generative Adversarial Loss

Recently, GANs have shown strong capability in learning image generative models. In the phase of training, the generative network  $G$  is trained to map samples from noise distribution  $p_z$  to real-world data distribution  $p_{data}$  through playing a minimax game with the discriminative network  $D$ . The discriminator  $D$  aims to distinguish the real samples  $x \sim p_{data}$  and the generated samples  $G(z) \sim p_g$  in the training procedure. And the generator  $G$  tries to confuse the discriminator  $D$  by generating more and more realistic samples. The process of this two-player minimax game can be formulated as

$$\min_G \max_D E_{x \sim \mathcal{X}} [\log D(x)] + E_{z \sim \mathcal{Z}} [\log (1 - D(G(z)))] \quad (6)$$

Therefore, we adapt the GANs learning strategy to remove ring artifacts in CBCT images as well. As shown in Fig.1, the generative network with the proposed smooth loss

$G_s$  is used to generate smooth image  $S(x)$ , given the input image  $x \in \mathcal{X}_{input}$ . Meanwhile, each input image  $x$  has a corresponding ground-truth image  $y_g$ . Suppose that all the target images  $y_g \in \mathcal{Y}_{without-artifacts}$  obey the distribution  $p_{real}$ , and then we expect the output images  $S(x)$  obey  $S(x) \sim p_{real}$ . A discriminative network  $D$  is additionally introduced based on the generative adversarial learning strategy, and the generative adversarial loss can be written as

$$\min_{G_s} \max_D E_{y_g \sim \mathcal{Y}} [\log D(y_g)] + E_{x \sim \mathcal{X}} [\log(1 - D(S(x)))] \quad (7)$$

### 2.3. Smooth Generative Adversarial Networks (SGAN)

Based on the aforementioned generative adversarial loss and the smooth loss, we introduce the SGAN to remove the ring artifacts from the original CBCT images. Inspired by the DC-GAN [15], we designed the SGAN composing of two modules: the image generative network with smooth loss  $G_s$  and the discriminative network  $D$  (Fig.1). Both the generative adversarial loss and the smooth loss are employed to train the SGAN.  $G_s$  and  $D$  play the two-player minimax game by optimizing different loss functions. Given a pair of data  $(x, y_g) \in (\mathcal{X}_{input}, \mathcal{Y}_{without-artifacts})$ , the loss function of image generative network  $G_s$  and the loss function of discriminative network  $D$  are formally defined as

$$G_s = \log[D(S(x)) - 1] + \left( \lambda_1 \sum_p (\partial_x S(x) - \partial_x y_g)^2 + \lambda_2 \sum_p (\partial_y S(x) - \partial_y y_g)^2 \right) \quad (8)$$

and

$$D = -\log[D(y_g)] - \log[D(S(x)) - 1] \quad (9)$$

respectively.

## 3. EXPERIMENTAL RESULTS

### 3.1. Experimental settings

We conducted experiments on both simulated and real data. These CBCT images are all gray scale and the values of all pixels were normalized to  $[0, 1]$ . The sizes of the images were set as  $100 \times 100$ . We updated the generative network with smooth loss  $G_s$  and the discriminative network  $D$ . Specifically, the SGD [16] solver with a learning rate of 0.001 and a first momentum of 0.5 was used in network training. The hyper-parameters  $\lambda_1 = 0.5$ ,  $\lambda_2 = 0.5$ , and the batch size of 64 was used.

To carry out comprehensive and fair comparisons, we compared the proposed method with three existing methods: the wavelet Fourier filtering (WF) [6], the ring correction in polar coordinate (RCP) [10] and the variation-based destriping model (VDM) [13]. These methods were realized using

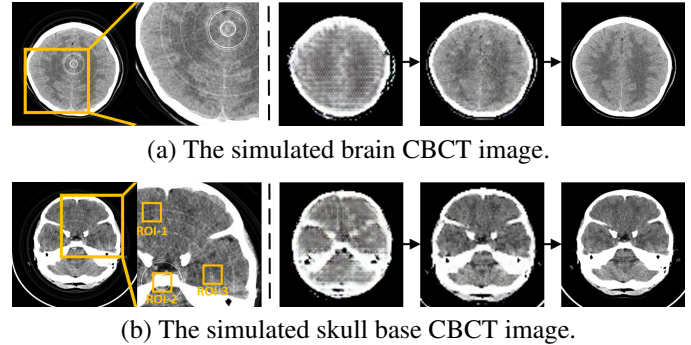


**Fig. 2.** Two simulated CBCT images and the generative processes of them.

the source codes from the original authors and each was run with default parameters. Our method was implemented in Caffe and all experiments are carried out on NVIDIA GeForce GTX 1080 Ti GPU with 32 GB RAM.

### 3.2. Experimental results and comparisons

**Qualitative evaluation:** We directly tested the proposed method on simulated data at first. We used two kinds of CBCT images as bases without artifacts, and simulated ring artifacts were superimposed on them to generate the corrupted images. The generated simulated data were used as the training set to train the whole network. Fig.2 shows some generative processes on the simulated brain CBCT images and the simulated skull base CBCT images. Our method generated the high-quality CBCT images without ring artifacts gradually from the simulated CBCT images after many iterations of training (Fig.2). Through introducing the smooth loss, the proposed SGAN removed more ring artifacts with less loss of image details.

In order to further verify the effectiveness of the proposed method, we also present the results on real CBCT images (Fig.3). Because the real CBCT images without ring artifacts are hard to acquire, visual inspection is probably an adequate approach to validate the removal of artifacts. From Fig.3, subfigure (a) are two original CBCT images whose contrasts were enhanced properly to make ring artifacts obvious. Subfigure (b) shows the whole result images obtained by the proposed method, where the ring artifacts are almost perfectly removed, and the image structures are well preserved. Subfigure (c) depicts the magnified portions of the original images, where some ring artifacts can be found clearly. Subfigure (d) shows the results processed by the WF, in which only ring artifacts at the center of images are corrected well, but some residual ring artifacts still exist away from the central location. Subfigure (e) gives the results processed by the RCP, where the details of images are basically preserved and most ring artifacts are effectively removed. However, this method needs to keep the balance between details preservation and

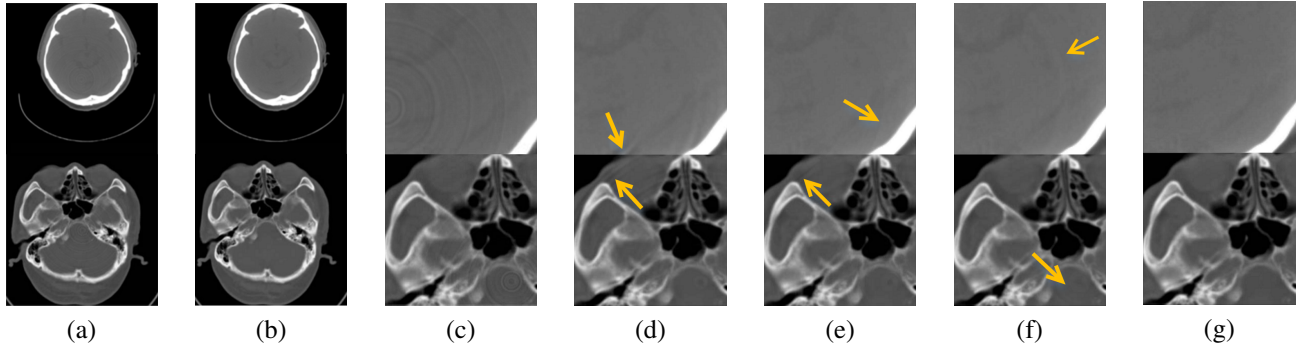


**Fig. 3.** Experimental results. (a) the real CBCT images with ring artifacts; (b) the resulting images by the proposed method; (c) the magnified regions of the real CBCT images with ring artifacts; (d) the magnified regions of the results by the WF; (e) the magnified regions of the results by the RCP; (f) the magnified regions of the results by the VDM; (g) the magnified regions of the results by the proposed method.

artifacts removal, such that residual ring artifacts are visible in some regions where the intensities of the artifacts are higher. From subfigure (f), the results processed by the VDM are not smooth enough in some regions, although no significant residual ring artifacts exist. As shown in subfigures (d)-(f), the residual ring artifacts are still visible in some regions indicated by yellow arrows. Subfigure (g) shows the results obtained by our proposed method. The proposed method effectively removed ring artifacts while preserving details and edges information of the CBCT images during smoothing. Meanwhile, as shown in Fig.4, the loss of the generator and the discriminator converges gradually.

**Quantitative evaluation:** We also used Peak Signal to Noise Ratio (PSNR) and Mean Structural Similarity (MSSIM) [17] as quantitative assessments. Table 1 shows the comparisons on PSNR and MSSIM for the different methods on the simulated skull base CBCT image. It can be observed that the proposed method retains the information of the original CBCT images to the largest extent.

**Table 1.** Comparison of PSNR and MSSIM for the different methods.

Methods	PSNR(dB)	MSSIM
WF	43.8253	0.9646
RCP	42.9617	0.9533
VDM	45.6575	0.9724
Proposed	<b>48.9887</b>	<b>0.9859</b>

Moreover, we introduced the block total variation (TV) and the block coefficient of variance (CV) [18] to measure local homogeneity and smoothness of images as in [13]. We chose three different representative blocks as ROIs in Fig.2 (b). The block TV and block CV indices calculated from the three ROIs are compared in Fig.5. The values of our proposed method are the closest to the base images.

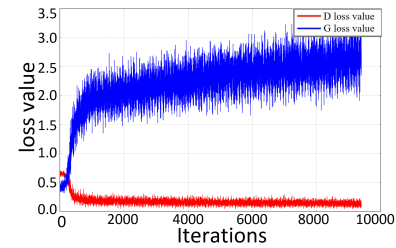


**Fig. 4.** The loss of both the generator and the discriminator.

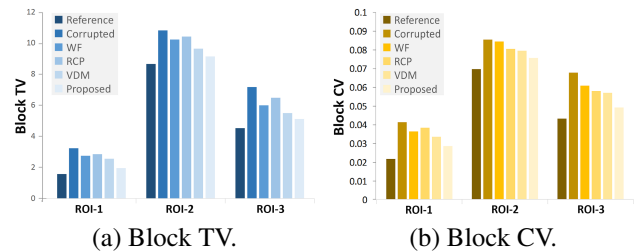


**Fig. 5.** The bar charts of the TV and CV of the ROIs marked in Fig.2(b).

## 4. CONCLUSIONS

This paper proposes the smooth generative adversarial networks (SGAN) to gradually remove ring artifacts in CBCT images. As a generic framework of learning mapping relationship between paired images, the SGAN combines the generative adversarial loss and the smooth loss as a novel training loss function. Simultaneously, an image generative network with smooth loss  $G_s$  is trained to narrow the discrepancy explored by the discriminative network  $D$ . Experimental results demonstrate that our method achieves excellent performance and it is superior to some other mainstream methods by both qualitative and quantitative assessment.

## 5. REFERENCES

- [1] F. Natterer and E. L. Ritman, "Past and future directions in x-ray computed tomography (CT)," *International Journal of Imaging Systems and Technology*, vol. 12, no. 4, pp. 175–187, 2002.
- [2] M. K. Hasan, F. Sadi, and S. Y. Lee, "Removal of ring artifacts in micro-CT imaging using iterative morphological filters," *Signal, Image and Video Processing*, vol. 6, no. 1, pp. 41–53, 2012.
- [3] A. C. Kak and M. Slaney, "Principles of computerized tomographic imaging," *Medical Physics*, vol. 29, no. 1, p. 22, 2001.
- [4] C. Raven, "Numerical removal of ring artifacts in microtomography," *Review of scientific instruments*, vol. 69, no. 8, pp. 2978–2980, 1998.
- [5] M. Boin and A. Haibel, "Compensation of ring artefacts in synchrotron tomographic images," *Optics express*, vol. 14, no. 25, pp. 12 071–12 075, 2006.
- [6] B. Münch, P. Trtik, F. Marone, and M. Stamparoni, "Stripe and ring artifact removal with combined waveletfourier filtering," *Optics express*, vol. 17, no. 10, pp. 8567–8591, 2009.
- [7] J. Sijbers and A. Postnov, "Reduction of ring artefacts in high resolution micro-CT reconstructions," *Physics in medicine and biology*, vol. 49, no. 14, p. N247, 2004.
- [8] F. Brun, G. Kourousias, D. Dreossi, and L. Mancini, "An improved method for ring artifacts removing in reconstructed tomographic images," in *World Congress on Medical Physics and Biomedical Engineering*. Springer, 2009, pp. 926–929.
- [9] Y. Kyriakou, D. Prell, and W. A. Kalender, "Ring artifact correction for high-resolution micro CT," *Physics in medicine and biology*, vol. 54, no. 17, p. N385, 2009.
- [10] D. Prell, Y. Kyriakou, and W. A. Kalender, "Comparison of ring artifact correction methods for flat-detector CT," *Physics in medicine and biology*, vol. 54, no. 12, p. 3881, 2009.
- [11] Y. Chen, G. Duan, A. Fujita, K. Hirooka, and Y. Ueno, "Ring artifacts reduction in cone-beam CT images based on independent component analysis," in *Instrumentation and Measurement Technology Conference*. IEEE, 2009, pp. 1734–1737.
- [12] Z. Wei, S. Wiebe, and D. Chapman, "Ring artifacts removal from synchrotron CT image slices," *Journal of Instrumentation*, vol. 8, no. 06, p. C6006, 2013.
- [13] L. Yan, T. Wu, S. Zhong, and Q. Zhang, "A variation-based ring artifact correction method with sparse constraint for flat-detector CT," *Physics in medicine and biology*, vol. 61, no. 3, p. 1278, 2016.
- [14] I. Goodfellow, J. Pouget-Abadie, M. Mirza, B. Xu, D. Warde-Farley, S. Ozair, A. Courville, and Y. Bengio, "Generative adversarial nets," in *Advances in neural information processing systems*, 2014, pp. 2672–2680.
- [15] A. Radford, L. Metz, and S. Chintala, "Unsupervised representation learning with deep convolutional generative adversarial networks," *arXiv preprint arXiv:1511.06434*, 2015.
- [16] S. Zhao and W. Li, "Fast asynchronous parallel stochastic gradient descent: A lock-free approach with convergence guarantee." in *AAAI*, 2016, pp. 2379–2385.
- [17] Z. Wang, A. C. Bovik, H. R. Sheikh, and E. P. Simoncelli, "Image quality assessment: from error visibility to structural similarity," *IEEE transactions on image processing*, vol. 13, no. 4, pp. 600–612, 2004.
- [18] U. Vovk, F. Pernus, and B. Likar, "A review of methods for correction of intensity inhomogeneity in CT," *IEEE transactions on medical imaging*, vol. 26, no. 3, pp. 405–421, 2007.